

Search for Stable Heavy Charged Particles in e^+e^- Collisions at $\sqrt{s} = 130\text{-}136, 161$ and 172 GeV

DELPHI Collaboration

Abstract

A search for stable or long-lived heavy charged particles in e^+e^- interactions at energies of 130-136, 161 and 172 GeV has been performed using the data taken by the DELPHI experiment at LEP. The search is based on particle identification provided by the Time Projection Chamber and the Ring Imaging Cherenkov detector. Upper limits at 95% confidence level are derived on the cross-section for heavy long-lived pair-produced charge $\pm e$ and $\pm 2/3e$ particles in the range of 0.4-2.3 pb for masses from 45 to 84 GeV/ c^2 . Within supersymmetric extensions of the Standard Model, long-lived charginos with masses from 45 to 84 (80) GeV/ c^2 for high (low) sneutrino masses can be excluded at 95% confidence level. Left-handed (right-handed) long-lived or stable smuons and staus with masses between 45 and 68 (65) GeV/ c^2 can be excluded at 95% confidence level.

(To be submitted to Physics Letters B)

P. Abreu²¹, W. Adam⁵⁰, T. Adye³⁷, I. Ajinenko⁴², G. D. Alekseev¹⁶, R. Alemany⁴⁹, P. P. Allport²², S. Almeded²⁴, U. Amaldi⁹, S. Amato⁴⁷, A. Andreatza²⁸, M. L. Andrieux¹⁴, P. Antilogus⁹, W. D. Apel¹⁷, B. Åsman⁴⁴, J.-E. Augustin²⁵, A. Augustinus⁹, P. Baillon⁹, P. Bambade¹⁹, F. Barao²¹, M. Barbi⁴⁷, G. Barbiellini⁴⁶, D. Y. Bardin¹⁶, G. Barker⁹, A. Baroncelli⁴⁰, O. Barring²⁴, J. A. Barrio²⁶, W. Bartl⁵⁰, M. J. Bates³⁷, M. Battaglia¹⁵, M. Baubillier²³, J. Baudot³⁹, K.-H. Becks⁵², M. Begalli⁶, P. Beilliere⁸, Yu. Belokopytov^{9,53}, K. Belous⁴², A. C. Benvenuti⁵, M. Berggren⁴⁷, D. Bertini²⁵, D. Bertrand², M. Besancon³⁹, F. Bianchi⁴⁵, M. Bigi⁴⁵, M. S. Bilenky¹⁶, P. Billoir²³, M.-A. Bizouard¹⁹, D. Bloch¹⁰, M. Blume⁵², T. Bolognese³⁹, M. Bonesini²⁸, W. Bonivento²⁸, P. S. L. Booth²², G. Borisov^{39,42}, C. Bosio⁴⁰, O. Botner⁴⁸, E. Boudinov³¹, B. Bouquet¹⁹, C. Bourdarios⁹, T. J. V. Bowcock²², M. Bozzo¹³, P. Branchini⁴⁰, K. D. Brand³⁶, T. Brenke⁵², R. A. Brenner¹⁵, C. Bricman², R. C. A. Brown⁹, P. Bruckman¹⁸, J.-M. Brunet⁸, L. Bugge³³, T. Buran³³, T. Burgsmueller⁵², P. Buschmann⁵², S. Cabrera⁴⁹, M. Caccia²⁸, M. Calvi²⁸, A. J. Camacho Rozas⁴¹, T. Camporesi⁹, V. Canale³⁸, M. Canepa¹³, K. Cankocak⁴⁴, F. Cao², F. Carena⁹, L. Carroll²², C. Caso¹³, M. V. Castillo Gimenez⁴⁹, A. Cattai⁹, F. R. Cavallo⁵, V. Chabaud⁹, Ph. Charpentier⁹, L. Chaussard²⁵, P. Checchia³⁶, G. A. Chelkov¹⁶, M. Chen², R. Chierici⁴⁵, P. Chliapnikov⁴², P. Chochula⁷, V. Chorowicz⁹, V. Cindro⁴³, P. Collins⁹, R. Contri¹³, E. Cortina⁴⁹, G. Cosme¹⁹, F. Cossutti⁴⁶, J.-H. Cowell²², H. B. Crawley¹, D. Crennell³⁷, G. Crosetti¹³, J. Cuevas Maestro³⁴, S. Czellar¹⁵, E. Dahl-Jensen²⁹, J. Dahm⁵², B. Dalmagne¹⁹, M. Dam²⁹, G. Damgaard²⁹, P. D. Dauncey³⁷, M. Davenport⁹, W. Da Silva²³, C. Defoix⁸, A. Deghorain², G. Della Ricca⁴⁶, P. Delpierre²⁷, N. Demaria³⁵, A. De Angelis⁹, W. De Boer¹⁷, S. De Brabandere², C. De Clercq², C. De La Vaissiere²³, B. De Lotto⁴⁶, A. De Min³⁶, L. De Paula⁴⁷, C. De Saint-Jean³⁹, H. Dijkstra⁹, L. Di Ciaccio³⁸, A. Di Diodato³⁸, F. Djama¹⁰, A. Djannati⁸, J. Dolbeau⁸, K. Doroba⁵¹, M. Dracos¹⁰, J. Drees⁵², K.-A. Drees⁵², M. Dris³², J.-D. Durand^{25,9}, D. Edsall¹, R. Ehret¹⁷, G. Eigen⁴, T. Ekelof⁴⁸, G. Eksping⁴⁴, M. Elsing⁹, J.-P. Engel¹⁰, B. Erzen⁴³, M. Espirito Santo²¹, E. Falk²⁴, D. Fassouliotis³², M. Feindt⁹, A. Fenyuk⁴², A. Ferrer⁴⁹, S. Fichet²³, T. A. Filippas³², A. Firestone¹, P.-A. Fischer¹⁰, H. Foeth⁹, E. Fokitis³², F. Fontanelli¹³, F. Formenti⁹, B. Franek³⁷, P. Frenkiel⁸, D. C. Fries¹⁷, A. G. Frodesen⁴, R. A. Garcia⁴⁹, F. Fulda-Quener¹⁹, J. Fuster⁴⁹, A. Galloni²², D. Gamba⁴⁵, M. Gandelman⁴⁷, C. Garcia⁴⁹, J. Garcia⁴¹, C. Gaspar⁹, U. Gasparini³⁶, Ph. Gavellet⁹, E. N. Gazis³², D. Gele¹⁰, J.-P. Gerber¹⁰, L. Gerdyukov⁴², R. Gokieli⁵¹, B. Golob⁴³, G. Gopal³⁷, L. Gorn¹, M. Gorski⁵¹, Yu. Gouz^{45,53}, V. Gracco¹³, E. Graziani⁴⁰, C. Green²², A. Grefrath⁵², P. Gris³⁹, G. Grosdidier¹⁹, K. Grzelak⁵¹, S. Gumenyuk^{28,53}, P. Gunnarsson⁴⁴, M. Gunther⁴⁸, J. Guy³⁷, F. Hahn⁹, S. Hahn⁵², Z. Hajduk¹⁸, A. Hallgren⁴⁸, K. Hamacher⁵², F. J. Harris³⁵, V. Hedberg²⁴, R. Henriques²¹, J. J. Hernandez⁴⁹, P. Herquet², H. Herr⁹, T. L. Hessing³⁵, J.-M. Heuser⁵², E. Higon⁴⁹, H. J. Hilke⁹, T. S. Hill¹, S.-O. Holmgren⁴⁴, P. J. Holt³⁵, D. Holthuisen³¹, S. Hoorelbeke², M. Houlden²², J. Hrubec⁵⁰, K. Huet², K. Hultqvist⁴⁴, J. N. Jackson²², R. Jacobsson⁴⁴, P. Jalochea¹⁸, R. Janik⁷, Ch. Jarlskog²⁴, G. Jarlskog²⁴, P. Jarry³⁹, B. Jean-Marie¹⁹, E. K. Johansson⁴⁴, L. Jonsson²⁴, P. Jonsson²⁴, C. Joram⁹, P. Juillot¹⁰, M. Kaiser¹⁷, F. Kapusta²³, K. Karafasoulis¹¹, M. Karlsson⁴⁴, E. Karvelas¹¹, S. Katsanevas³, E. C. Katsoufis³², R. Keranen⁴, Yu. Khokhlov⁴², B. A. Khomenko¹⁶, N. N. Khovanski¹⁶, B. King²², N. J. Kjaer³¹, O. Klapp⁵², H. Klein⁹, A. Klovning⁴, P. Kluit³¹, P. Kokkinos¹¹, A. Konopliannikov⁴², M. Koratzinos⁹, K. Korcyl¹⁸, V. Kostoukhine⁴², C. Kourkoumelis³, O. Kouznetsov^{13,16}, M. Krammer⁵⁰, C. Kreuter⁹, I. Kronkvist²⁴, Z. Krumstein¹⁶, W. Krupinski¹⁸, P. Kubinec⁷, W. Kuczewicz¹⁸, K. Kurvinen¹⁵, C. Lacasta⁴⁹, I. Laktineh²⁵, J. W. Lamsa¹, L. Lanceri⁴⁶, D. W. Lane¹, P. Langefeld⁵², J.-P. Laugier³⁹, R. Lauhakangas¹⁵, G. Leder⁵⁰, F. Ledroit¹⁴, V. Lefebvre², C. K. Legan¹, R. Leitner³⁰, J. Lemonne², G. Lenzen⁵², V. Lepeltier¹⁹, T. Lesiak¹⁸, J. Libby³⁵, D. Liko⁹, R. Lindner⁵², A. Lipniacka⁴⁴, I. Lippi³⁶, B. Loerstad²⁴, J. G. Loken³⁵, J. M. Lopez⁴¹, D. Loukas¹¹, P. Lutz³⁹, L. Lyons³⁵, J. MacNaughton⁵⁰, G. Maehlum¹⁷, J. R. Mahon⁶, T. G. M. Malmgren⁴⁴, V. Malychhev¹⁶, F. Mandl⁵⁰, J. Marco⁴¹, R. Marco⁴¹, B. Marechal⁴⁷, M. Margoni³⁶, J.-C. Marin⁹, C. Mariotti⁹, A. Markou¹¹, C. Martinez-Rivero³⁴, F. Martinez-Vidal⁴⁹, S. Marti i Garcia²², F. Matorras⁴¹, C. Matteuzzi²⁸, G. Matthiae³⁸, M. Mazzucato³⁶, M. Mc Cubbin²², R. Mc Kay¹, R. Mc Nulty²², J. Medbo⁴⁸, M. Merk³¹, C. Meroni²⁸, S. Meyer¹⁷, W. T. Meyer¹, M. Michelotto³⁶, E. Migliore⁴⁵, L. Mirabito²⁵, W. A. Mitaroff⁵⁰, U. Mjoernmark²⁴, T. Moe⁴⁴, R. Moeller²⁹, K. Moenig⁹, M. R. Monge¹³, P. Moretti¹³, H. Mueller¹⁷, K. Muenich⁵², M. Mulders³¹, L. M. Mundim⁶, W. J. Murray³⁷, B. Muryn^{14,18}, G. Myatt³⁵, F. Naraghi¹⁴, F. L. Navarria⁵, S. Navas⁴⁹, K. Nawrocki⁵¹, P. Negri²⁸, S. Nemecek¹², W. Neumann⁵², N. Neumeister⁵⁰, R. Nicolaidou³, B. S. Nielsen²⁹, M. Nieuwenhuizen³¹, V. Nikolaenko¹⁰, P. Niss⁴⁴, A. Nomerotski³⁶, A. Normand³⁵, M. Novak¹², W. Oberschulte-Beckmann¹⁷, V. Obraztsov⁴², A. G. Olshevski¹⁶, A. Onofre²¹, R. Orava¹⁵, K. Osterberg¹⁵, A. Ouraou³⁹, P. Paganini¹⁹, M. Paganoni^{9,28}, P. Pages¹⁰, R. Pain²³, H. Palka¹⁸, Th. D. Papadopoulou³², K. Papageorgiou¹¹, L. Pape⁹, C. Parkes³⁵, F. Parodi¹³, A. Passeri⁴⁰, M. Pegoraro³⁶, L. Peralta²¹, M. Pernicka⁵⁰, A. Perrotta⁵, C. Petridou⁴⁶, A. Petrolini¹³, H. T. Phillips³⁷, G. Piana¹³, F. Pierre³⁹, M. Pimenta²¹, T. Podobnik⁴³, O. Podobrin⁹, M. E. Pol⁶, G. Polok¹⁸, P. Poropat⁴⁶, V. Pozdniakov¹⁶, P. Privitera³⁸, N. Pukhaeva¹⁶, A. Pullia²⁸, D. Radojicic³⁵, S. Ragazzi²⁸, H. Rahmani³², J. Rames¹², P. N. Ratoff²⁰, A. L. Read³³, M. Reale⁵², P. Rebecchi¹⁹, N. G. Redaelli²⁸, M. Regler⁵⁰, D. Reid⁹, R. Reinhardt⁵², P. B. Renton³⁵, L. K. Resvanis³, F. Richard¹⁹, J. Richardson²², J. Ridky¹², G. Rinaudo⁴⁵, I. Ripp³⁹, A. Romero⁴⁵, I. Roncagliolo¹³, P. Ronchese³⁶, L. Roos²³, E. I. Rosenberg¹, P. Roudeau¹⁹, T. Rovelli⁵, V. Ruhlmann-Kleider³⁹, A. Ruiz⁴¹, K. Rybicki¹⁸, H. Saarikko¹⁵, Y. Sacquin³⁹, A. Sadovsky¹⁶, O. Sahr¹⁴, G. Sajot¹⁴, J. Salt⁴⁹, J. Sanchez²⁶, M. Sannino¹³, M. Schimmelpfennig¹⁷, H. Schneider¹⁷, U. Schwickerath¹⁷, M. A. E. Shellyns⁵², G. Sciolla⁴⁵, F. Scuri⁴⁶, P. Seager²⁰, Y. Sedykh¹⁶, A. M. Segar³⁵, A. Seitz¹⁷, R. Sekulin³⁷, L. Serbelloni³⁸, R. C. Shellard⁶, P. Siegrist³⁹, R. Silvestre³⁹, S. Simonetti³⁹, F. Simonetto³⁶, A. N. Sisakian¹⁶, B. Sitar⁷, T. B. Skaali³³, G. Smadja²⁵, N. Smirnov⁴², O. Smirnova²⁴, G. R. Smith³⁷, O. Solovianov⁴², R. Sosnowski⁵¹, D. Souza-Santos⁶, T. Spassov²¹, E. Spiriti⁴⁰, P. Sponholz⁵², S. Squarcia¹³, D. Stampfer⁹, C. Stanescu⁴⁰, S. Stanic⁴³, S. Stapnes³³, I. Stavitski³⁶, K. Stevenson³⁵, A. Stocchi¹⁹, J. Strauss⁵⁰, R. Strub¹⁰, B. Stugu⁴, M. Szczekowski⁵¹, M. Szeptycka⁵¹,

T. Tabarelli²⁸, J.P. Tavernet²³, E. Tcherniaev⁴², J. Thomas³⁵, A. Tilquin²⁷, J. Timmermans³¹, L.G. Tkatchev¹⁶, T. Todorov¹⁰, S. Todorova¹⁰, D.Z. Toet³¹, A. Tomaradze², B. Tome²¹, A. Tonazzo²⁸, L. Tortora⁴⁰, G. Tranströmer²⁴, D. Treille⁹, G. Tristram⁸, A. Trombini¹⁹, C. Troncon²⁸, A. Tsirou⁹, M.-L. Turluer³⁹, I.A. Tyapkin¹⁶, M. Tyndel³⁷, S. Tzamarias²², B. Ueberschär⁵², O. Ullaland⁹, V. Uvarov⁴², G. Valenti⁵, E. Vallazza⁹, C. Vander Velde², G.W. Van Apeldoorn³¹, P. Van Dam³¹, W.K. Van Doninck², J. Van Eldik³¹, A. Van Lysebetten², N. Vassilopoulos³⁵, G. Vegni²⁸, L. Ventura³⁶, W. Venus³⁷, F. Verbeure², M. Verlato³⁶, L.S. Vertogradov¹⁶, D. Vilanova³⁹, P. Vincent²⁵, L. Vitale⁴⁶, A.S. Vodopyanov¹⁶, V. Vrba¹², H. Wahlen⁵², C. Walck⁴⁴, M. Weierstall⁵², P. Weilhammer⁹, C. Weiser¹⁷, A.M. Wetherell⁹, D. Wicke⁵², J.H. Wickens², M. Wielers¹⁷, G.R. Wilkinson⁹, W.S.C. Williams³⁵, M. Winter¹⁰, M. Witek¹⁸, T. Wlodek¹⁹, K. Woschnagg⁴⁸, K. Yip³⁵, O. Yushchenko⁴², F. Zach²⁵, A. Zaitsev⁴², A. Zalewska⁹, P. Zalewski⁵¹, D. Zavrtnik⁴³, E. Zevgolatakos¹¹, N.I. Zimin¹⁶, M. Zito³⁹, D. Zontar⁴³, G.C. Zucchelli⁴⁴, G. Zumerle³⁶

¹Department of Physics and Astronomy, Iowa State University, Ames IA 50011-3160, USA

²Physics Department, Univ. Instelling Antwerpen, Universiteitsplein 1, B-2610 Wilrijk, Belgium and IIHE, ULB-VUB, Pleinlaan 2, B-1050 Brussels, Belgium

and Faculté des Sciences, Univ. de l'Etat Mons, Av. Maistriau 19, B-7000 Mons, Belgium

³Physics Laboratory, University of Athens, Solonos Str. 104, GR-10680 Athens, Greece

⁴Department of Physics, University of Bergen, Allégaten 55, N-5007 Bergen, Norway

⁵Dipartimento di Fisica, Università di Bologna and INFN, Via Irnerio 46, I-40126 Bologna, Italy

⁶Centro Brasileiro de Pesquisas Físicas, rua Xavier Sigaud 150, RJ-22290 Rio de Janeiro, Brazil and Depto. de Física, Pont. Univ. Católica, C.P. 38071 RJ-22453 Rio de Janeiro, Brazil

and Inst. de Física, Univ. Estadual do Rio de Janeiro, rua São Francisco Xavier 524, Rio de Janeiro, Brazil

⁷Comenius University, Faculty of Mathematics and Physics, Mlynska Dolina, SK-84215 Bratislava, Slovakia

⁸Collège de France, Lab. de Physique Corpusculaire, IN2P3-CNRS, F-75231 Paris Cedex 05, France

⁹CERN, CH-1211 Geneva 23, Switzerland

¹⁰Centre de Recherche Nucléaire, IN2P3 - CNRS/ULP - BP20, F-67037 Strasbourg Cedex, France

¹¹Institute of Nuclear Physics, N.C.S.R. Demokritos, P.O. Box 60228, GR-15310 Athens, Greece

¹²FZU, Inst. of Physics of the C.A.S. High Energy Physics Division, Na Slovance 2, 180 40, Praha 8, Czech Republic

¹³Dipartimento di Fisica, Università di Genova and INFN, Via Dodecaneso 33, I-16146 Genova, Italy

¹⁴Institut des Sciences Nucléaires, IN2P3-CNRS, Université de Grenoble 1, F-38026 Grenoble Cedex, France

¹⁵Research Institute for High Energy Physics, SEFT, P.O. Box 9, FIN-00014 Helsinki, Finland

¹⁶Joint Institute for Nuclear Research, Dubna, Head Post Office, P.O. Box 79, 101 000 Moscow, Russian Federation

¹⁷Institut für Experimentelle Kernphysik, Universität Karlsruhe, Postfach 6980, D-76128 Karlsruhe, Germany

¹⁸Institute of Nuclear Physics and University of Mining and Metallurgy, Ul. Kawory 26a, PL-30055 Krakow, Poland

¹⁹Université de Paris-Sud, Lab. de l'Accélérateur Linéaire, IN2P3-CNRS, Bât. 200, F-91405 Orsay Cedex, France

²⁰School of Physics and Chemistry, University of Lancaster, Lancaster LA1 4YB, UK

²¹LIP, IST, FCUL - Av. Elias Garcia, 14-1º, P-1000 Lisboa Codex, Portugal

²²Department of Physics, University of Liverpool, P.O. Box 147, Liverpool L69 3BX, UK

²³LPNHE, IN2P3-CNRS, Universités Paris VI et VII, Tour 33 (RdC), 4 place Jussieu, F-75252 Paris Cedex 05, France

²⁴Department of Physics, University of Lund, Sölvegatan 14, S-22363 Lund, Sweden

²⁵Université Claude Bernard de Lyon, IPNL, IN2P3-CNRS, F-69622 Villeurbanne Cedex, France

²⁶Universidad Complutense, Avda. Complutense s/n, E-28040 Madrid, Spain

²⁷Univ. d'Aix - Marseille II - CPP, IN2P3-CNRS, F-13288 Marseille Cedex 09, France

²⁸Dipartimento di Fisica, Università di Milano and INFN, Via Celoria 16, I-20133 Milan, Italy

²⁹Niels Bohr Institute, Blegdamsvej 17, DK-2100 Copenhagen 0, Denmark

³⁰NC, Nuclear Centre of MFF, Charles University, Areal MFF, V Holesovickach 2, 180 00, Praha 8, Czech Republic

³¹NIKHEF, Postbus 41882, NL-1009 DB Amsterdam, The Netherlands

³²National Technical University, Physics Department, Zografou Campus, GR-15773 Athens, Greece

³³Physics Department, University of Oslo, Blindern, N-1000 Oslo 3, Norway

³⁴Dpto. Física, Univ. Oviedo, Avda. Calvo Sotelo, S/N-33007 Oviedo, Spain, (CICYT-AEN96-1681)

³⁵Department of Physics, University of Oxford, Keble Road, Oxford OX1 3RH, UK

³⁶Dipartimento di Fisica, Università di Padova and INFN, Via Marzolo 8, I-35131 Padua, Italy

³⁷Rutherford Appleton Laboratory, Chilton, Didcot OX11 0QX, UK

³⁸Dipartimento di Fisica, Università di Roma II and INFN, Tor Vergata, I-00173 Rome, Italy

³⁹CEA, DAPNIA/Service de Physique des Particules, CE-Saclay, F-91191 Gif-sur-Yvette Cedex, France

⁴⁰Istituto Superiore di Sanità, Ist. Naz. di Fisica Nucl. (INFN), Viale Regina Elena 299, I-00161 Rome, Italy

⁴¹Instituto de Física de Cantabria (CSIC-UC), Avda. los Castros, S/N-39006 Santander, Spain, (CICYT-AEN96-1681)

⁴²Inst. for High Energy Physics, Serpukov P.O. Box 35, Protvino, (Moscow Region), Russian Federation

⁴³Department of Astroparticle Physics, School of Environmental Sciences, Nova Gorica, and J. Stefan Institute, Ljubljana, Slovenia

⁴⁴Fysikum, Stockholm University, Box 6730, S-113 85 Stockholm, Sweden

⁴⁵Dipartimento di Fisica Sperimentale, Università di Torino and INFN, Via P. Giuria 1, I-10125 Turin, Italy

⁴⁶Dipartimento di Fisica, Università di Trieste and INFN, Via A. Valerio 2, I-34127 Trieste, Italy

and Istituto di Fisica, Università di Udine, I-33100 Udine, Italy

⁴⁷Univ. Federal do Rio de Janeiro, C.P. 68528 Cidade Univ., Ilha do Fundão BR-21945-970 Rio de Janeiro, Brazil

⁴⁸Department of Radiation Sciences, University of Uppsala, P.O. Box 535, S-751 21 Uppsala, Sweden

⁴⁹IFIC, Valencia-CSIC, and D.F.A.M.N., U. de Valencia, Avda. Dr. Moliner 50, E-46100 Burjassot (Valencia), Spain

⁵⁰Institut für Hochenergiephysik, Österr. Akad. d. Wissensch., Nikolsdorfergasse 18, A-1050 Vienna, Austria

⁵¹Inst. Nuclear Studies and University of Warsaw, Ul. Hoza 69, PL-00681 Warsaw, Poland

⁵²Fachbereich Physik, University of Wuppertal, Postfach 100 127, D-42097 Wuppertal, Germany

⁵³On leave of absence from IHEP Serpukhov

1 Introduction

A search for stable or long-lived charged particles[†] produced in e^+e^- collisions has been performed using the data taken by the DELPHI experiment at the Large Electron Positron Collider (LEP) running at centre-of-mass energies of $\sqrt{s} = 130$ -136, 161 and 172 GeV. The result extends the searches carried out at 91 GeV [1] to masses above 45 GeV/ c^2 .

Although in the Standard Model (SM) no further fundamental stable heavy particle is expected to exist, it is important to search for new physics since it is generally accepted that the Standard Model is not a complete theory. One possibility to extend the Standard Model is Supersymmetry (SUSY). It predicts the existence of new particles, some of which might be accessible at LEP II [2]. It is usually assumed that the lightest supersymmetric particle (LSP) is stable and neutral. Most of the supersymmetric particles will decay through cascades into the LSP and Standard Model particles. However, it is not excluded that some of the charged supersymmetric particles have sufficiently long lifetimes to be observed as stable particles in the detector. In models where the neutralino is the LSP, this situation can occur for charginos if the light chargino and the LSP are almost degenerate. In models where the gravitino is the LSP [3], sleptons can obtain long lifetimes in a very natural way [4], especially the staus, the superpartners of the tau lepton.

Apart from these theoretical motivations, it is important to study the LEP II data and look for unexpected particles such as stable heavy charged particles with charge $\pm e$ and stable fractional charged particles from unconfined quarks with charge $\pm 2/3e$. Therefore, a search has been made for stable heavy charged particles with a mass larger than 45 GeV/ c^2 and charges $\pm e$ or $\pm 2/3e$ that decay outside the tracking detectors, which extend to a typical radius of 1.5 m. The search assumes that new long-lived charged particles do not interact more strongly than ordinary matter particles, i.e. electrons, muons, pions, kaons and protons. No search was made for charge $\pm 1/3e$ particles, because the main tracking detector is not sensitive to their low ionization loss.

The search is based on the ionization loss measurement in the main tracking device of DELPHI, the Time Projection Chamber (TPC), and particle identification provided by the Barrel Ring Imaging Cherenkov detector (RICH). For heavy particles with masses above 45 GeV/ c^2 , no Cherenkov photons are expected in the gas or liquid radiator. The combination of the TPC and RICH detectors allows for an efficient detection of new heavy particles with a small background from ordinary matter particles. The data taken in 1995 correspond to a total integrated luminosity of 5.9 pb⁻¹ at centre-of-mass energies of 130-136 GeV, while the data taken in 1996 correspond to 9.8 pb⁻¹ at 161 GeV and 9.9 pb⁻¹ at 172 GeV[‡].

2 Event and track selection

A detailed description of the DELPHI apparatus can be found in [5] and its performance in [6]. The event selection was mainly based on the TPC and optimised for both low and high multiplicity events. Events with initial state radiation and a resonant Z were kept in the sample. Tracks were selected if their impact parameter in the transverse plane was less than 5 cm and in the longitudinal direction less than 10 cm. The relative error on the measured momentum was required to be less than 100% and the track length

[†]Throughout the paper stable particles include long-lived particles decaying outside the detector.

[‡]This includes 1.0 pb⁻¹ taken at 170 GeV

larger than 30 cm. Each event was divided into two hemispheres according to the thrust axis calculated from charged and neutral particles. The total momentum of all the particles in each hemisphere was required to be more than 10 GeV/c. An event was accepted if it had at least one charged particle with a momentum above 5 GeV/c reconstructed on the basis of the TPC and lying inside the Barrel RICH acceptance of $|\cos \theta| < 0.68$, where θ is the polar angle. To remove cosmic muons, tighter cuts were applied on the impact parameter of 0.15 cm in the transverse and 1.5 cm in the longitudinal direction for events with two tracks, at least one of which had one or more associated hits in the barrel muon chambers. Thus 2068 events were selected for the 130-136 GeV data set, 1795 events for the 161 GeV data set and 1441 for the 172 GeV data set.

The analysis was optimised to select high mass particles with charge $\pm e$ or $\pm 2/3e$, combining the particle identification provided by the TPC and RICH. The cuts explained in detail below are indicated in Figures 1 to 3.

To ensure a reliable measurement of the normalised ionization loss dE/dx in the TPC, at least 80 wire signals (out of the maximum of 192) were required. The average resolution for particles with momenta above 5 GeV/c is better than 10%. The ionization loss was normalised to that of a minimum ionising particle. It was calibrated on a run-to-run basis and cross-checked with identified particles in the RICH detector. Results for the ionization loss for different particles as a function of the momentum can be found in [6].

Two dE/dx selections were applied to search for tracks with anomalous ionization.

Firstly, charged particles with momenta [§] above 5 GeV/c and normalised ionization losses above 2 and below 10 were selected to look for particles with low velocity βc . For ionization losses above 10, the TPC becomes inefficient due to saturation and splitting effects. For particles with a β below 0.1, and hence ionization losses well above 10, the global tracking efficiency is further reduced because the track elements in the different tracking detectors appear to be displaced and rotated.

Secondly, particles with momenta above 15 GeV/c with ionization losses below the expected ionization for a proton by more than 0.3 units were selected, to look for $\pm 2/3e$ particles with high β .

Cherenkov radiation data from the gas and liquid radiators of the Barrel RICH [7] were then used. The average Cherenkov angle was estimated from single photons associated to a track, as described in [6] and [8]. The mean number of photons for a $\beta = 1$ particle was 14 in the liquid radiator and 8 in the gas radiator. Both radiators were used in the veto mode.

In the gas radiator, it was required that no photons were associated to the track. Data taken when the Barrel RICH was not operational were rejected. It was checked on a track-by-track basis that the detector was fully operational by requiring that more than two ionization hits, associated to the track, were detected in the multiwire proportional chamber of the RICH. The pion, kaon and proton thresholds in the gas radiator are at $\sim 2, 8$ and 15 GeV/c. Consequently the gas veto strongly reduced the number of ordinary matter particles accepted. The gas veto was applied for particles with momenta above 5 GeV/c.

In the liquid radiator, it was required that not more than 4 photons were associated to the track. The cut was placed at four and not at zero photons, because photons are searched for in a large area, so backgrounds from rings and ionization hits from neighbouring particles can be present. In this way, particles with a β of less than 0.79 were selected. The liquid veto was applied for tracks with momenta above 15 GeV/c, corresponding to masses of 12 GeV/c² and higher.

[§]In the following, "momentum" means the apparent momentum, defined as the momentum divided by the charge $|q|$, because this is the physical quantity measured (from the track curvature).

It is important to reduce the background of cosmic muons. There were about 23 cosmic rays in the total event sample. For cosmic muons, no Cherenkov light is detected in the upper half of the detector, so they look like heavy particles. Therefore only tracks in the bottom half of the detector - corresponding to azimuthal angles larger than π - were used for the liquid veto.

By combining the measurement of the ionization loss with the gas veto and by combining the gas and liquid veto, clean signatures for high mass particles were obtained.

Summarising, tracks were selected if they had no associated photons in the gas RICH and satisfied any of the following further criteria:

- (i) for momenta above 5 GeV/c, the measured normalised ionization loss was anomalously high - above 2 and below 10;
- (ii) above 15 GeV/c, the measured ionization loss was anomalously low - below the proton expectation by at least 0.3 units;
- (iii) above 15 GeV/c, and for azimuthal angles larger than π , not more than four photons were detected in the liquid RICH.

Selection (ii) was designed for charge $\pm 2/3e$ particles.

Comparing the ionization loss measurement and the liquid veto RICH signal before and after the gas veto was applied allowed the background or misidentification probability to be estimated and compared to simulations. For the simulation of the physics background, the PYTHIA generator [9] with DELPHI tuning [10] was used in combination with a detailed simulation program for the detector response [6].

3 Experimental Results

In Figures 1, 2 and 3, the measured normalised energy loss and Cherenkov angle in the liquid RICH after the gas veto are shown as a function of the momentum for the 130-136, 161, and 172 GeV data. The straight lines indicate the selections, and expectation curves for different masses and charges are also shown. After applying the selections, described in the previous section, no candidate particles were found. This is compatible with the expected background estimated below.

The expected background with dE/dx above 2 comes from overlapping tracks, delta rays and the tail of the Landau distribution. It is reduced by the gas veto to only 0.5 ± 0.2 events after selection (i), for the total data set.

The background expected after selection (ii) comes mainly from protons, kaon and pions. It is reduced by the gas veto to 0.3 ± 0.3 events for the whole data set.

The background passing selection (iii) comes from the fact that there is a probability of about 7% of observing four photons or less in the liquid radiator for ordinary matter particles. The expected background amounts to 2 ± 1 events for the whole data set.

Figures 1b, 2b and 3b contain some entries corresponding to charged particles with a Cherenkov angle more than 50 mrad below the saturated angle of 670 mrad. These particles are mostly misidentified pions, usually with few photons in the ring, where the Cherenkov angle is shifted downwards due to tails in the single photon distribution. These tails are well reproduced by the simulation program.

To obtain upper limits on the cross-section, simulation studies were performed for charge $\pm e$ and $\pm 2/3e$ particles. Efficiencies were obtained for different mass values ranging from 45 to 84 GeV/ c^2 and different centre-of-mass energies.

A possible signal of stable, heavy pair-produced charged particles was simulated using the SUSYGEN generator [11] including initial state radiation, resulting in an almost flat

distribution in $\cos\theta$. Particles of different mass and charge were generated and followed through the detector, simulating its detailed response. The efficiency for different heavy particle masses and centre-of-mass energies is given in Figure 4a. The efficiency drops rapidly to zero for masses above 65 (77, 84) GeV/c^2 for a centre-of-mass energy of 136 (161, 172) GeV , mainly because the normalised dE/dx exceeds 10 for higher mass values.

The same procedure was followed for particles with charge $\pm 2/3e$, and the efficiencies are given in Figure 4b. The valley seen in Figure 4b around masses of 60 and 70 GeV/c^2 is caused by the fact that the dE/dx curve for a high mass particle of charge $\pm 2/3e$ crosses the pion expectation band. An analysis based only on the ionization loss measurement would have holes in the efficiency curves for a charge $\pm 2/3e$ particle. For a charge $\pm e$ particle, the efficiency would be significantly reduced in the mass region from 45 to 55 GeV/c^2 . Use of the liquid and gas RICH veto largely avoids this problem.

The quoted efficiencies can be extrapolated to cases where, for example, the pair produced particles have an angular distribution of the form $1 + \cos^2\theta$, as for SM fermion pairs, or cases where ordinary fragmentation particles accompany the heavy particle. In the first case the efficiency would be reduced by 16%.

From the efficiencies obtained from simulation, upper limits on the cross-section at 95% confidence level were obtained. The results for the different energies are shown in Figure 5 for charge $\pm e$ and $\pm 2/3e$ particles. Upper limits in the range of 0.4 to 2.3 pb on the cross-section for pair-produced heavy particles with charge $\pm e$ or $\pm 2/3e$ are obtained in the mass region from 45 to 84 GeV/c^2 .

4 Implications for SUSY models

In supersymmetric extensions of the Standard Model with a minimal Higgs sector (MSSM), R-parity conservation, and a neutralino as the LSP, the next-to-lightest sparticle (NLSP) can have a long lifetime provided that it has sufficiently high mass degeneracy with the LSP and that the couplings are small. In the following, such models with a long-lived chargino or slepton as the NLSP are discussed and mass limits are given. In the special scenario where the chargino is the NLSP and a slepton is highly degenerate with it, the mass limits derived for the charginos can also be applied for the slepton.

Another class of models assumes that the gravitino is the LSP. In a number of these models sleptons, in particular staus, may have sufficiently long lifetimes in a very natural way, so that they should be visible as stable charged particles in the detector [3]. For selectrons, the contribution via t -channel neutralino exchange has to be taken into account. For certain values of the parameters of the MSSM, the predicted production cross-section falls below 0.1 pb; hence no general mass limit can be set.

4.1 Charginos

If the second lightest SUSY particle is a chargino and it has a sufficiently long lifetime, it cannot be found by the usual chargino searches [12], since they assume immediate decay of the particle, leaving characteristic signatures with high missing energy. However, if the decay length of the chargino exceeds several metres, it is visible in the detector. This case is covered by this search.

In the Minimal Supersymmetric Standard Model (MSSM), the chargino and the neutralino masses are determined by the low energy mass scale parameters for the bino, M_1 , and the wino, M_2 , by the low energy scale parameter of the Higgs terms in the supersymmetric lagrangian, μ , and by the ratio of the vacuum expectation values, $\tan\beta = v_2/v_1$.

For given values of M_2 , μ and $\tan\beta$, the chargino masses are fully determined, whereas M_1 enters in the neutralino mixing matrix. A random variation of the parameters of the model was performed for low ($\tan\beta=1.5$) and high ($\tan\beta=35$) values of $\tan\beta$, and the mass spectrum, production cross-sections and decay widths were calculated using the SUSYGEN program. The lifetime of the light chargino was estimated from its total decay width, taking into account all possible decay channels. Points in parameter space were selected for which the light chargino was heavier than $45 \text{ GeV}/c^2$ and its decay probability within a flight distance larger than 1.5 m was larger than 95%, to ensure that the efficiency curve of Figure 4a could be applied.

In experimental analyses the validity of the GUT relation $M_1 = 5/3 \tan^2 \theta_W M_2$ is usually assumed [2]. Within such models, high degeneracies of the light chargino with the LSP are possible if $M_2 \gg |\mu|$. M_2 must have a value well above $10 \text{ TeV}/c^2$ to get sufficiently long-lived charginos. In this case the mass of the light chargino, which is an almost pure Higgsino, is given by $|\mu|$. The production cross-section does not depend on the sneutrino mass, and a lower limit of $84 \text{ GeV}/c^2$ on the mass of these long-lived charginos can be given.

In order to cover a larger range of models, the GUT relation was dropped, and the parameters were varied within the bounds $0.5 \leq M_1/M_2 \leq 16$, $0 \text{ GeV}/c^2 < M_2 \leq 200 \text{ GeV}/c^2$, and $-1500 \text{ GeV}/c^2 \leq \mu \leq 1500 \text{ GeV}/c^2$. For most of the solutions, the mass difference between the LSP and the chargino was less than $0.1 \text{ GeV}/c^2$. Again, the scans were carried out for $\tan\beta = 1.5$ and $\tan\beta = 35$. All other sparticle masses were chosen at a scale of one TeV, with the exception of the sneutrino mass, $m_{\tilde{\nu}}$. Since for all selected parameter settings the relation $|\mu| \gg M_2$ holds, resulting in a light chargino that is mostly a wino, a low sneutrino mass can reduce the production cross-section via destructive interference of the t -channel $\tilde{\nu}$ contribution with the s -channel Z/γ contribution. For this reason, the cases of a high sneutrino mass ($200 \text{ GeV}/c^2 < m_{\tilde{\nu}} < 1 \text{ TeV}/c^2$) and a light sneutrino mass ($41 \text{ GeV}/c^2 \leq m_{\tilde{\nu}} \leq 200 \text{ GeV}/c^2$) were considered separately.

Figure 6 shows the dependence of the production cross-sections on the chargino mass for a centre-of-mass energy of 172 GeV. The experimental upper limits on the production cross-sections at $\sqrt{s}=130$ -136 GeV, $\sqrt{s}=161$ GeV, and $\sqrt{s}=172$ GeV were combined, taking into account the ratio of the expected production cross-sections for long-lived charginos at these energies[¶]. This ratio was calculated as a function of the chargino mass and, at each mass, the most conservative case was taken. The combined experimental upper limit on stable chargino production is shown in Figure 6. For high (low) sneutrino masses, long-lived charginos can be excluded up to masses of 84 (80) GeV/c^2 at 95% confidence level. Figure 7 indicates the regions of the parameter space for which charginos have long lifetimes.

4.2 Sleptons

In a similar way, sleptons can also acquire a long lifetime within the framework of the MSSM. The results are interpreted for the case where the NLSP is a smuon or a stau.

Both left-handed and right-handed sleptons can decay into a neutralino and the corresponding lepton. If the slepton mass is sufficiently high to produce on-shell final state particles, this decay is usually fast and the lifetime of the sleptons is short. However, if the slepton mass is too small to produce the final state lepton, the decay is kinematically forbidden, and smuons (staus) must decay via virtual muon (tau) exchange into lighter

[¶]The upper limit at 95% confidence level is given by the formula $\sigma_{exp} < 3/(\epsilon_1 L_1 \sigma_{1,th} / \sigma_{3,th} + \epsilon_2 L_2 \sigma_{2,th} / \sigma_{3,th} + \epsilon_3 L_3)$, where σ_{exp} is the combined experimental upper limit, ϵ_i and L_i are the efficiencies and integrated luminosities, and $\sigma_{i,th}$ is the expected theoretical production cross-section at the three different energies.

particles. As a consequence, the decay is highly suppressed and the slepton acquires a long lifetime. Figure 8 shows the production cross-sections for left- and right-handed smuons at a centre-of-mass energy of 172 GeV, estimated with the SUSYGEN generator. They are also valid for staus in the limiting case of no mixing.

The production cross-sections depend only on the mass of the slepton. This allowed the experimental upper limits on the production cross-sections for the different energies to be combined, by taking into account the ratios between the expected production cross-sections for long-lived sleptons (as a function of their mass) at the different energies. The resulting combined experimental upper limit is indicated in Figure 8. For left-handed (right-handed) long-lived smuons and staus, masses between 45 and 68(65) GeV/ c^2 can be excluded at 95% confidence level. The same mass limits hold for the case where one of the sleptons is the LSP, which is not favoured since a charged stable LSP would build stable atoms, which have not been observed [13].

The slepton can also have a long lifetime in some regions of the MSSM where the chargino is the NLSP and one slepton is a bit heavier than the light chargino. The left-handed smuon (stau) can decay into the chargino and a muon (tau) neutrino. Therefore a high smuon (stau) lifetime is only possible for a very high mass degeneracy ($\Delta m < 1$ keV/ c^2) with the chargino. In addition the mass difference between the slepton and the LSP must be smaller than the lepton mass; otherwise, the slepton decays immediately into the lepton and the LSP. Thus for smuons, the mass difference between the chargino and the LSP needs to be smaller than the muon mass and the chargino becomes long-lived. In this case the mass limits for long-lived charginos given in Figure 6 should be applied. In a similar way, staus can decay outside the detector if the mass difference between the stau and the LSP is smaller than 0.01 GeV/ c^2 . As in the previous case, the light chargino is long-lived, and the appropriate mass limits are valid.

5 Summary

A search for stable or long-lived heavy charged particles in e^+e^- interactions at energies of 130-136, 161 and 172 GeV has been performed. No candidates were observed.

Upper limits at 95% confidence level are given for the cross-section of pair produced charge $\pm e$ and $\pm 2/3e$ particles in the range of 0.4-2.3 pb for masses from 45 to 84 GeV/ c^2 . Within the framework of the MSSM and assuming that the neutralino is the LSP, limits at 95% confidence level are derived for long-lived charginos and sleptons. Long-lived charginos with masses ranging from 45 to 84(80) GeV/ c^2 for high (low) sneutrino masses are excluded. For selectrons no general mass limits can be given. Left-handed (right-handed) long-lived or stable smuons and staus with masses between 45 and 68(65) GeV/ c^2 are excluded.

6 Acknowledgements

We are greatly indebted to our technical collaborators and funding agencies for their support and to the members of the CERN accelerator divisions for the excellent performance of the LEP collider in this new energy regime.

References

- [1] P. Abreu et al. (DELPHI Collaboration), Phys. Lett. **B247** (1990) 157;
P. Abreu et al. (DELPHI Collaboration), CERN-PPE/90-167;
D. Buskulic et al. (ALEPH Collaboration), Phys. Lett. **B303** (1993) 198;
R. Akers et al. (OPAL Collaboration), Zeit. Phys. **C67** (1995) 203.
- [2] H. P. Nilles, Phys. Rep. **110** (1984) 1;
H.E. Haber and J.L. Kane, Phys. Rep. **117** (1985) 75;
W. de Boer et al., Z. Phys. **C71** (1996) 415;
W. de Boer et al., *MSSM predictions of the Neutral Higgs Boson Masses and LEP-II Production Cross-Sections*, hep-ph/9603346.
- [3] S. Ambrosanio, G. L. Kane, G. D. Kribs, S. P. Martin, S. Mrenna, Phys. Rev. Lett. **76** (1996) 3498;
S. Ambrosanio, G. L. Kane, G. D. Kribs, S. P. Martin, S. Mrenna, Phys. Rev. **D54** (1996) 5395;
J. L. Lopez, D.V. Nanopoulos, Mod. Phys. Lett. **A10** (1996) 2473;
J. L. Lopez, D.V. Nanopoulos, hep-ph/9608275.
- [4] M. Dine et al., Phys. Rev. Lett. **76** (1996) 3484;
S. Dimopoulos et al., SLAC-PUB-7236, hep-ph/9607450.
- [5] P. Aarnio et al., Nucl. Instr. Meth. **A303** (1991) 233.
- [6] P. Abreu et al., Nucl. Instr. Meth. **A378** (1996) 57.
- [7] W. Adam et al., Nucl. Instr. Meth. **A343** (1994) 1.
- [8] W. Adam et al., Nucl. Instr. Meth. **A343** (1994) 240;
M. Battaglia and P. M. Kluit, *Particle Identification using the RICH detectors based on the RIBMEAN package*, DELPHI note 96-133 RICH 90.
- [9] T. Sjöstrand, Comp. Phys. Comm. **39** (1986) 347;
T. Sjöstrand, *PYTHIA 5.6 and JETSET 7.3*, CERN-TH/6488/92.
- [10] P. Abreu et al. (DELPHI Collaboration), CERN-PPE 96-120, to be published in Zeit. Phys. C.
- [11] S. Katsanevas and S. Melanchroinos in *Physics at LEP2*, CERN 96-01 (Vol.2) 328.
- [12] D. Buskulic et al. (ALEPH Collaboration), Phys. Lett. **B373** (1996) 246;
G. Alexander et al. (OPAL Collaboration), Phys. Lett. **B377** (1996) 181;
P. Abreu et al. (DELPHI Collaboration), Phys. Lett. **B382** (1996) 323.
- [13] E.W. Kolb, M.S. Turner, *The early universe*, Addison-Wesley (1990).

DELPHI searches at 130-136 GeV

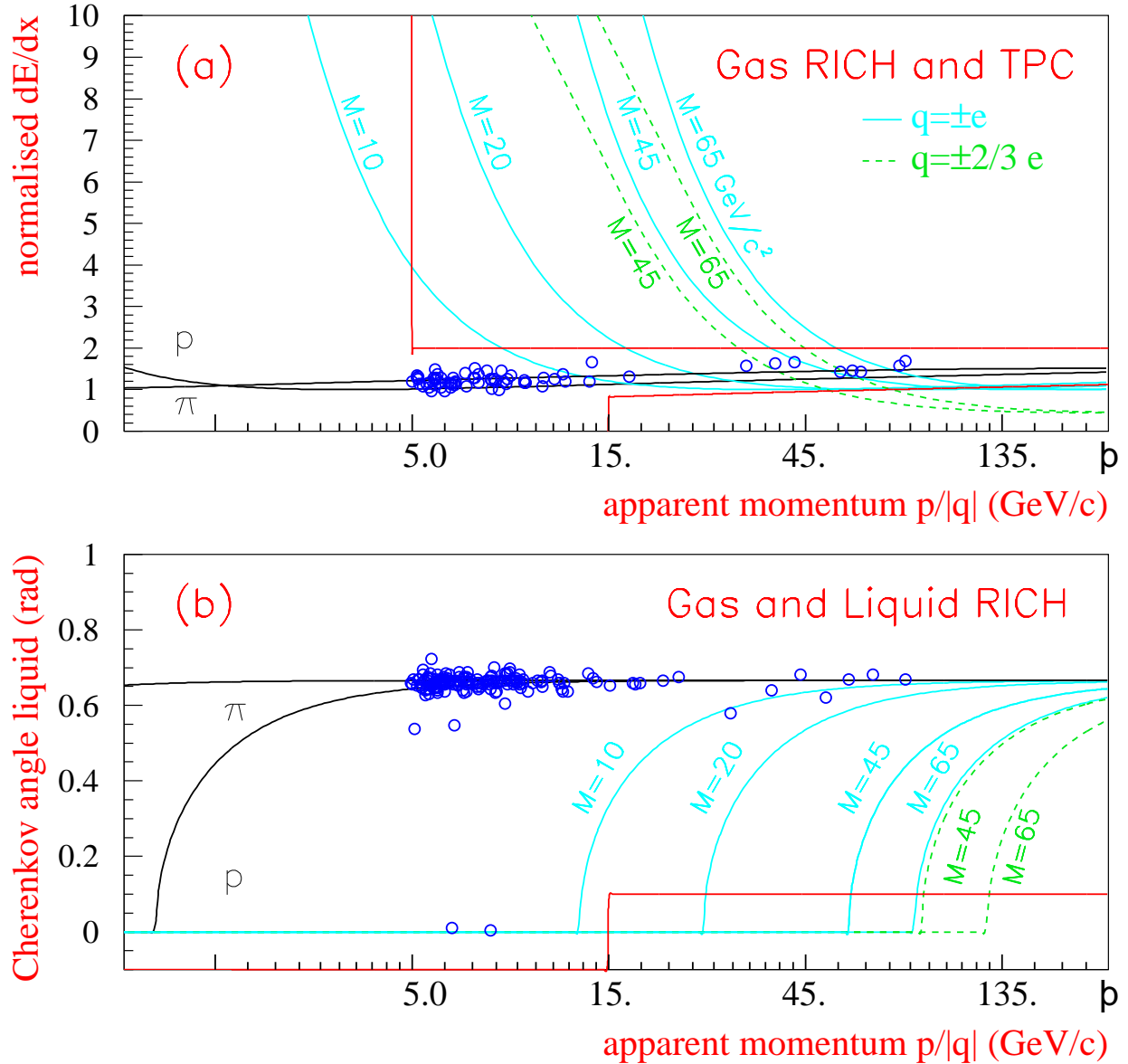


Figure 1: (a) Normalised energy loss as a function of the apparent momentum $p/|q|$ after the gas veto for the 130-136 GeV data. (b) Measured Cherenkov angle in the liquid radiator as a function of the apparent momentum after the gas veto: if four photons or less were observed in the liquid radiator, the Cherenkov angle was set equal to zero. The expectation curves for charge $\pm e$ particles for pions, protons and heavy particles with masses of 10, 20, 45 and 65 GeV/c^2 are given, as well as the dashed curves for charge $\pm 2/3 e$ particles with masses of 45 and 65 GeV/c^2 . The rectangular areas in (a) indicate selections (i) and (ii), and that in (b) shows selection (iii). The selection criteria are explained in section 2.

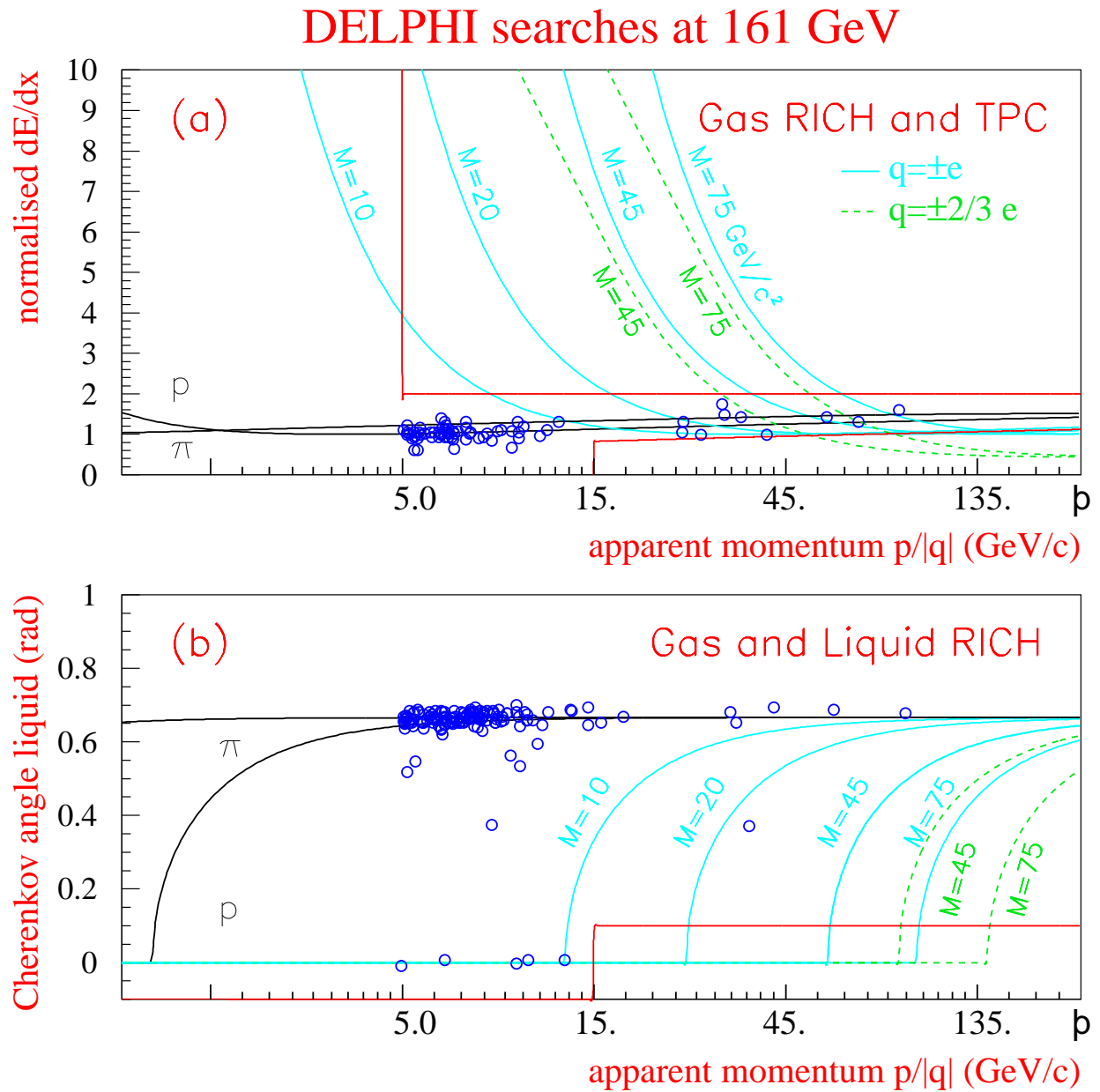


Figure 2: Same as Figure 1 but for the 161 GeV data.

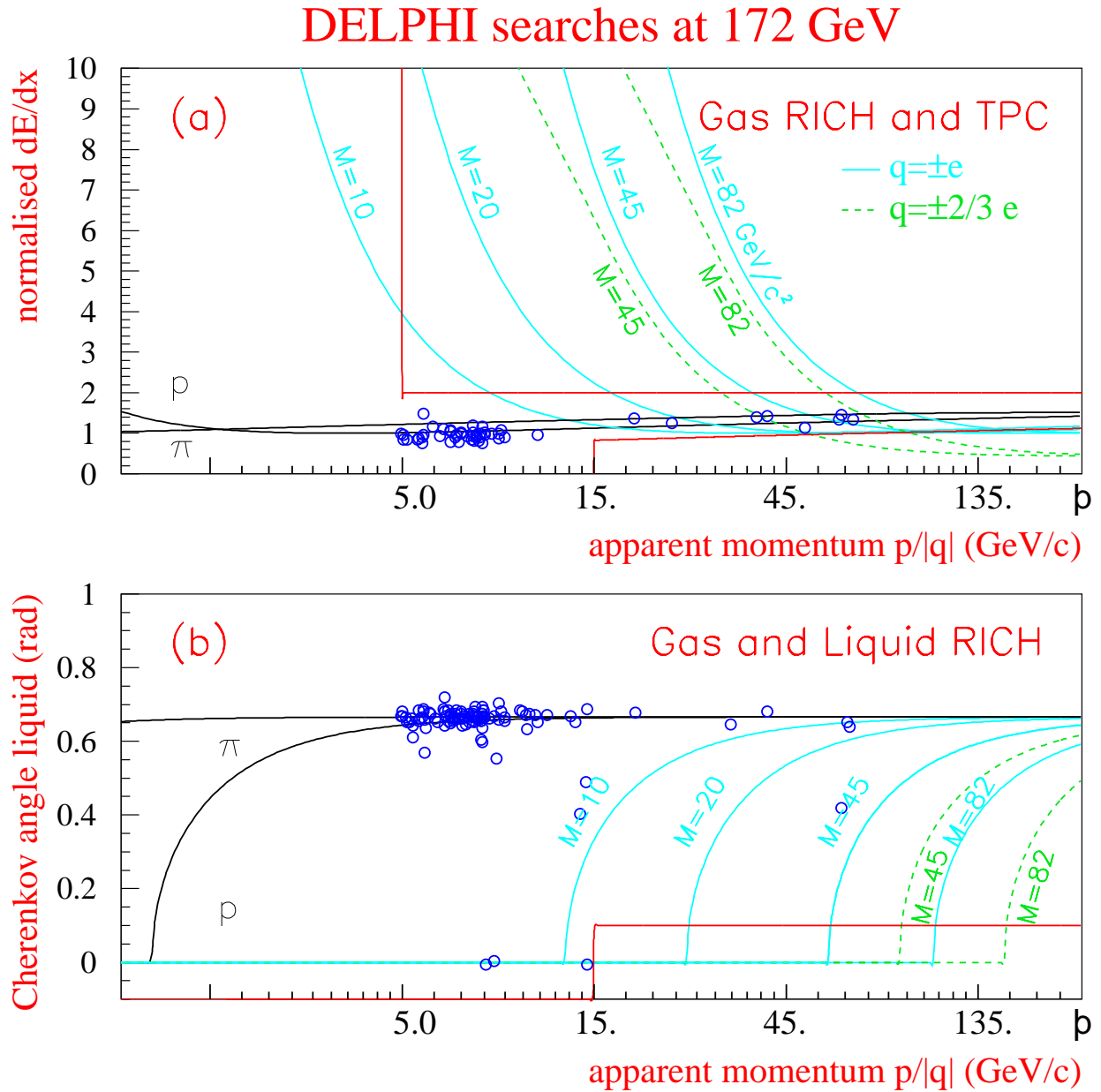


Figure 3: Same as Figure 1 but for the 172 GeV data.

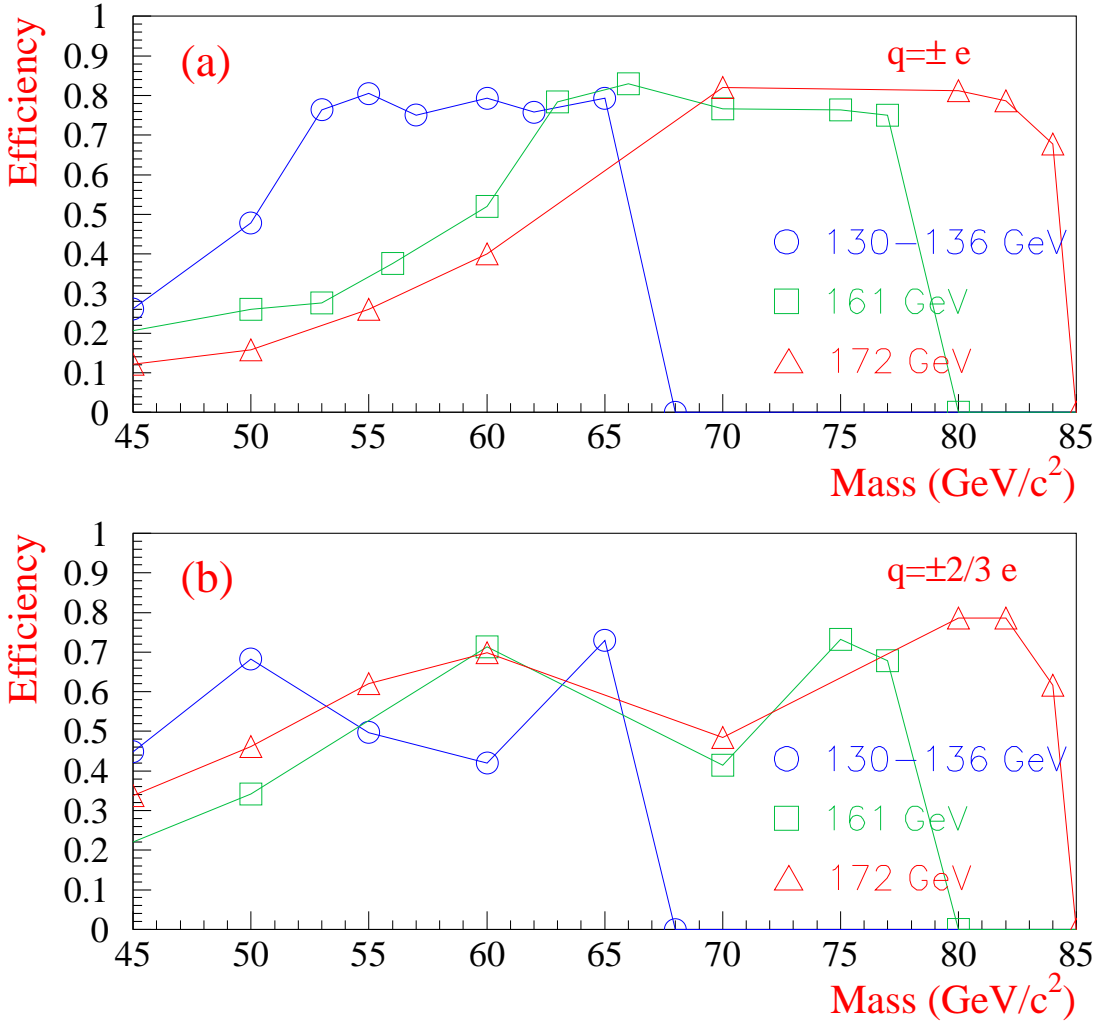


Figure 4: (a) Efficiency for pair-produced heavy particles as a function of the mass of the particle for centre-of-mass energies of 130–136 (circles), 161 (rectangles), and 172 GeV (triangles) charge $\pm e$ particles, interpolated with solid lines. (b) Same quantities for charge $\pm 2/3e$ particles.

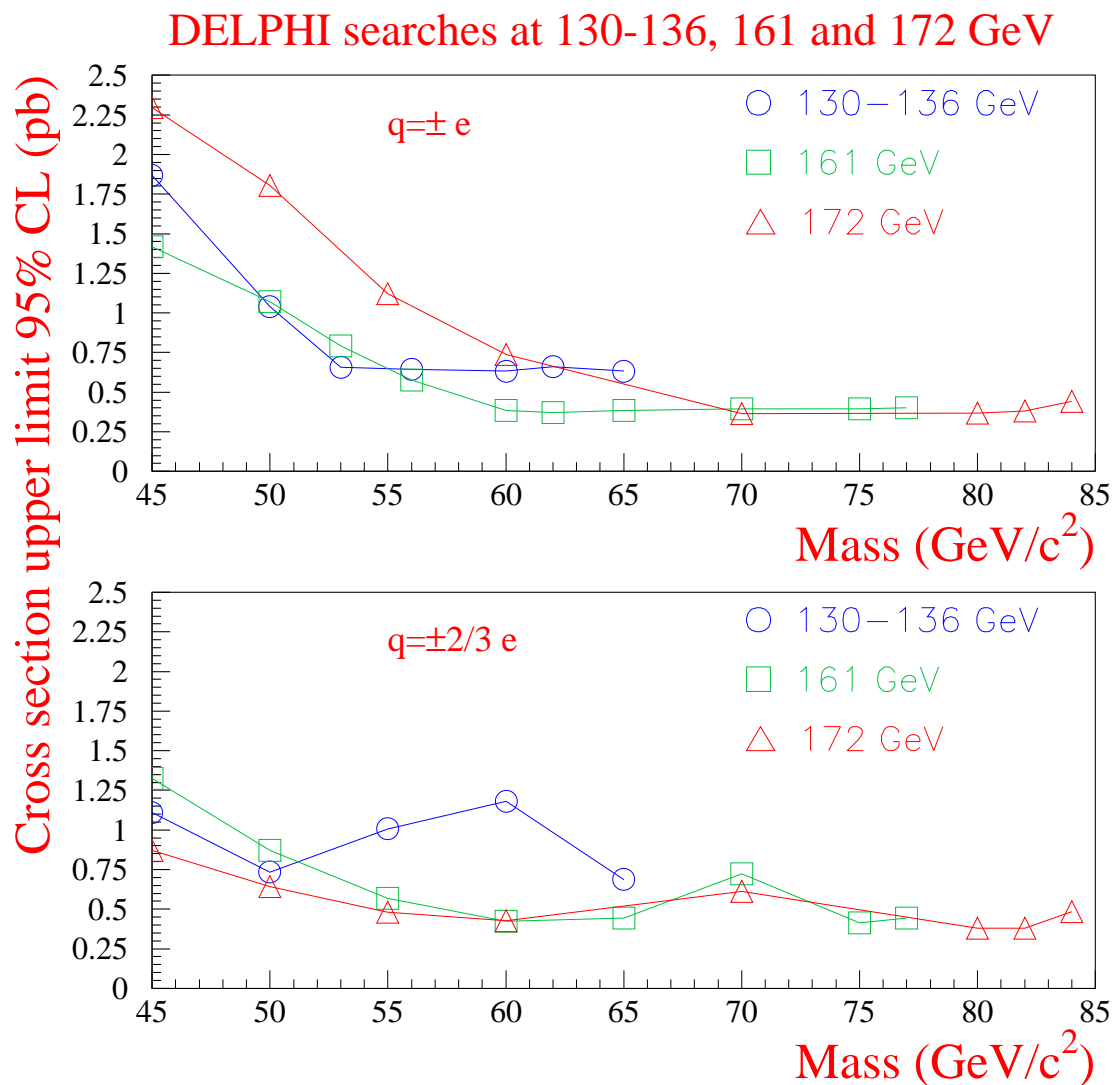


Figure 5: Cross-section upper limit at 95% confidence level for pair-produced heavy particles as a function of the mass of the particle for centre-of-mass energies of 130-136 (circles), 161 (rectangles) and 172 (triangles) GeV, separately for particles of charge $\pm e$ (upper plot) and $\pm 2/3 e$ (lower plot).

DELPHI Mass Limits on Stable Charginos

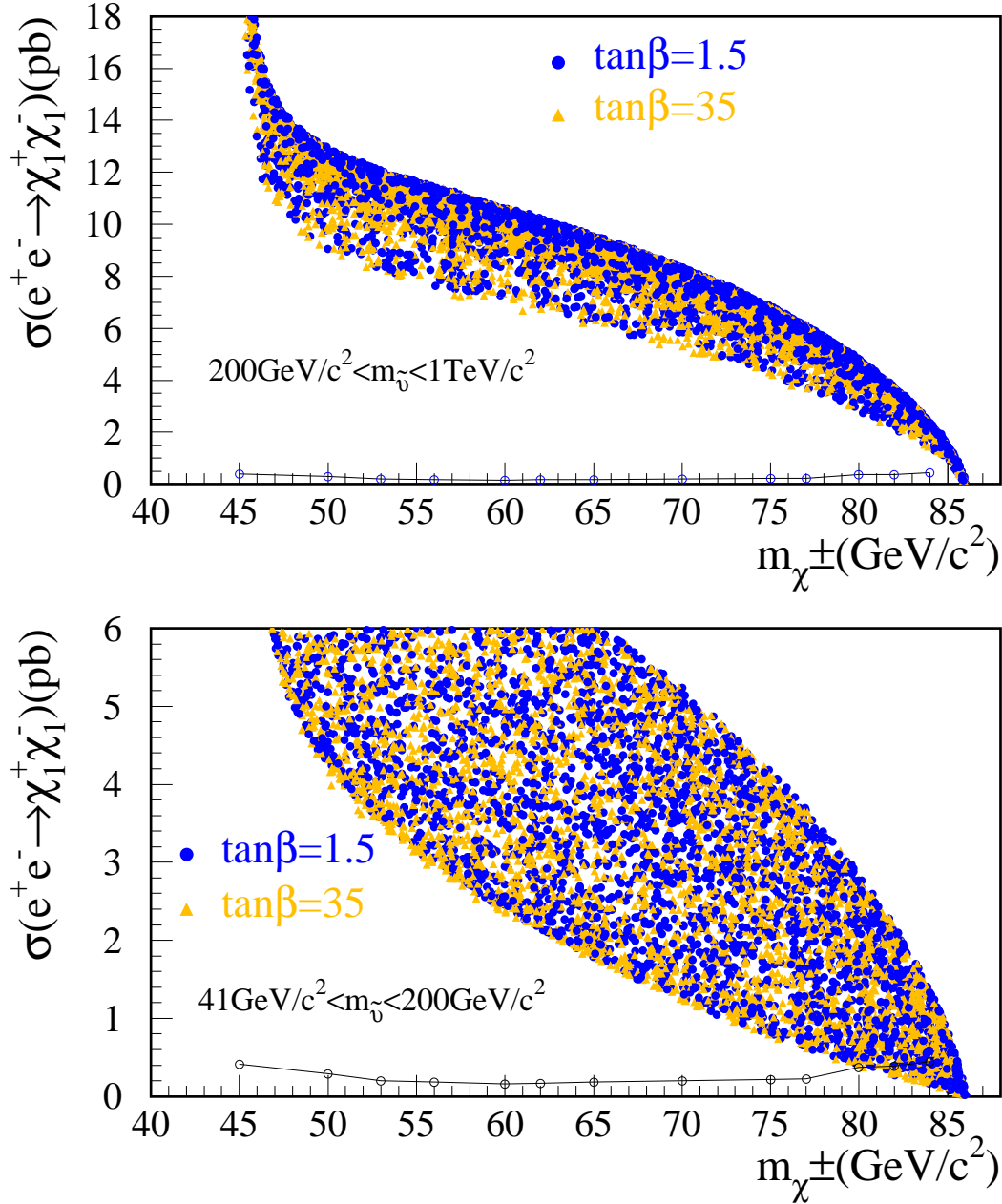


Figure 6: Production cross-section for charginos with long lifetimes at a centre-of-mass energy of 172 GeV for high and low sneutrino masses and two values of $\tan\beta$, obtained with the SUSYGEN generator. The dark points (lighter triangles) show the predicted cross-sections for low (high) values of $\tan\beta$ for values of the MSSM parameters M_1 , M_2 , μ , and the sneutrino mass $m_{\tilde{\nu}}$ within the ranges given in the text. The lines connecting the open circles correspond to the combined experimental upper limit on the cross-section at 95% confidence level, as explained in section 4.1. Stable charginos up to 84 (80) GeV/c^2 can be excluded for high (low) sneutrino masses.

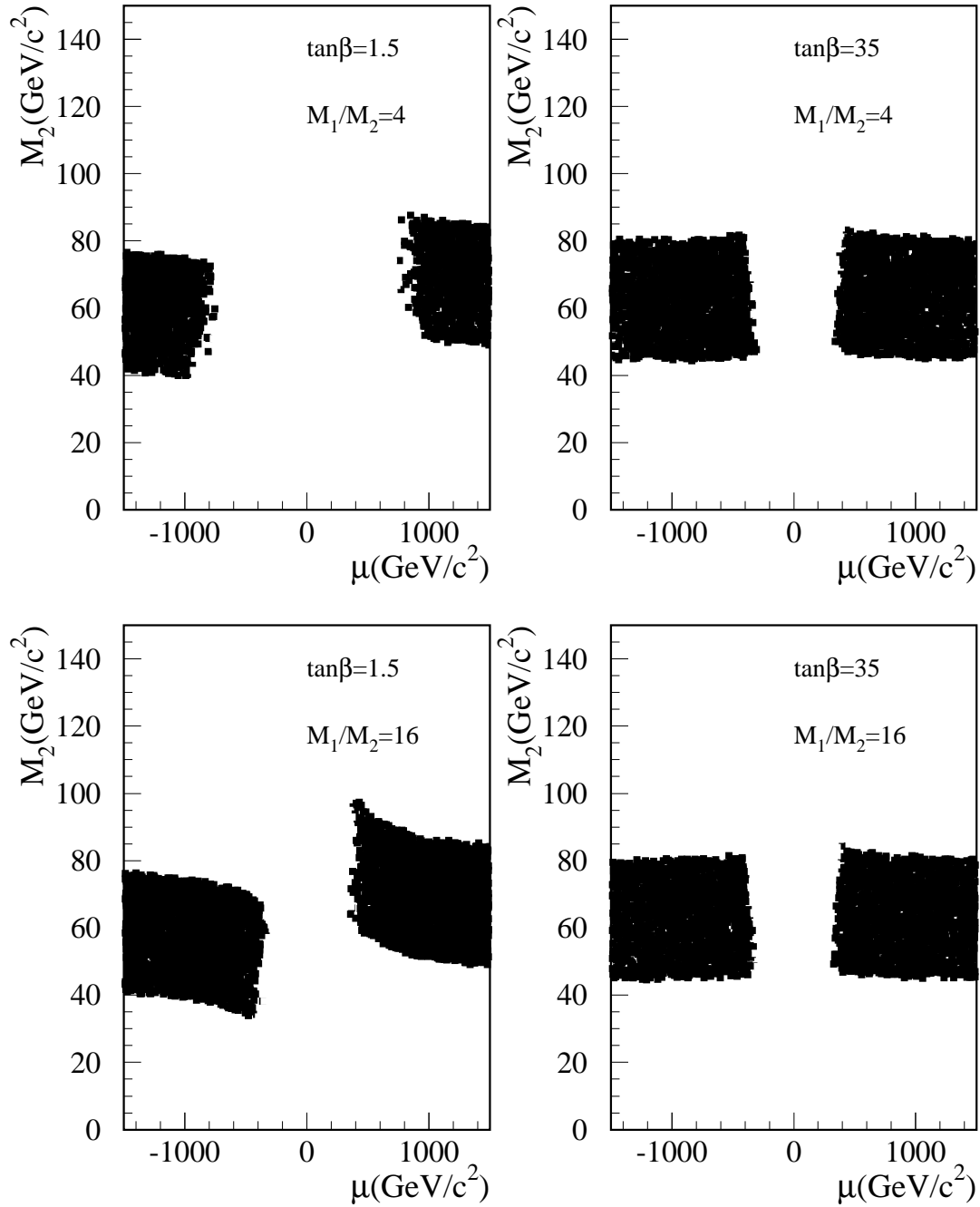


Figure 7: Regions of the parameter space in which long-lived charginos with masses higher than the LEP I limit of 45 GeV/c² are possible, for $\tan\beta = 1.5$ and $\tan\beta = 35$. The ratio M_1/M_2 was fixed at 4 (upper figures) and 16 (lower figures).

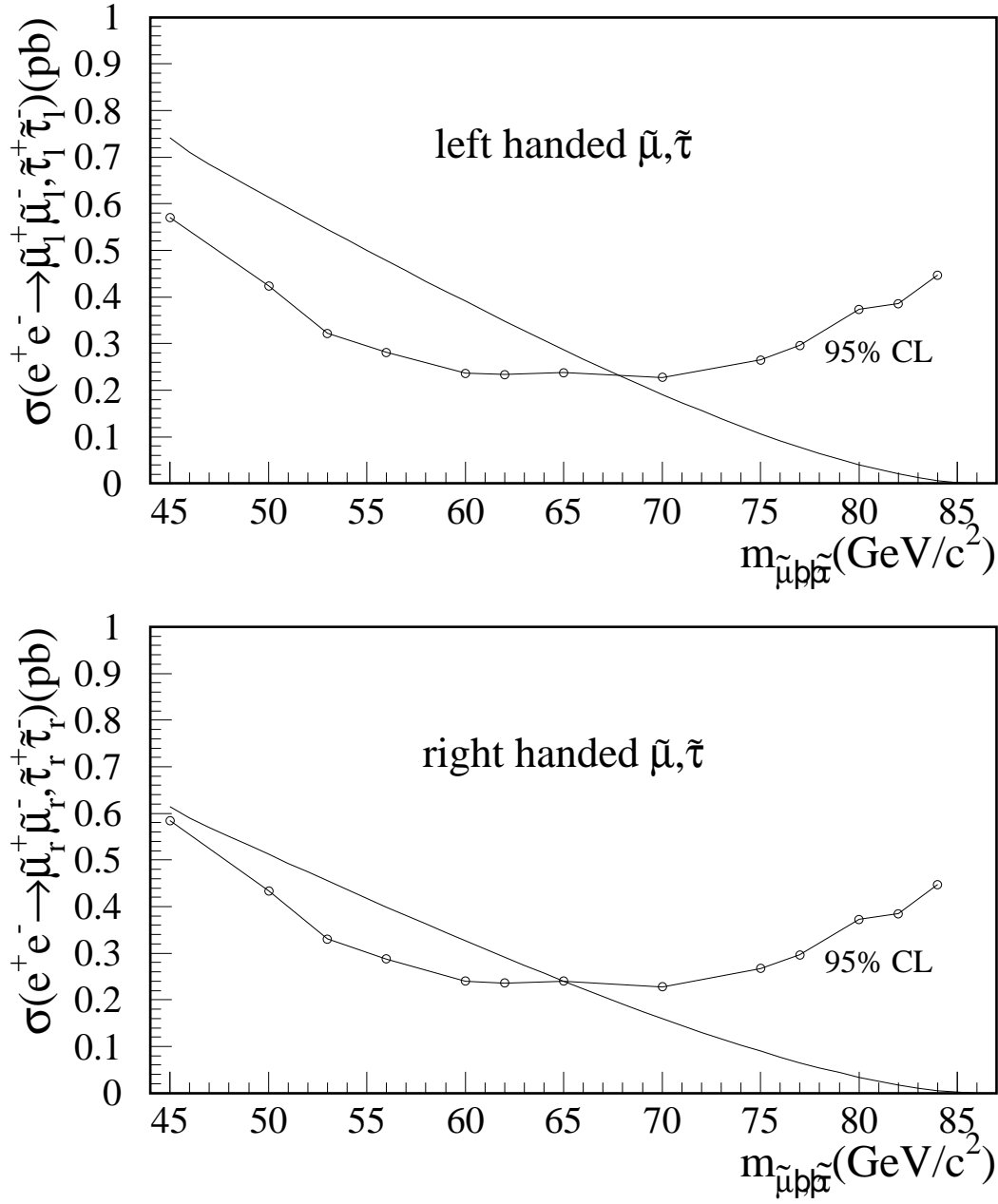


Figure 8: Production cross-section for stable or long-lived left-handed (upper plot) and right-handed (lower plot) smuons or staus at a centre-of-mass energy of 172 GeV, calculated with SUSYGEN. The lines connecting the open circles indicate the combined experimental upper limit on the production cross-section at 95% confidence level, as explained in section 4.2. Masses between 45 GeV/c² and 68 (65) GeV/c² can be excluded for left-handed (right-handed) smuons and staus.